Repulsive $1/r^3$ interaction

Bo Gao
Department of Physics and Astronomy, University of Toledo, Toledo, Ohio 43606
(Received 3 November 1998)

Analytic solutions of the Schrödinger equation are presented for a repulsive $1/r^3$ potential. They lead to an in-depth understanding of scattering by a pure repulsive $1/r^3$ interaction including exact cross sections and phase shifts. Scattering by any potential which is asymptotically a repulsive $1/r^3$ is also discussed. [S1050-2947(99)03704-X]

PACS number(s): 34.10.+x, 34.50.−s, 32.80.Pj, 03.65.−w

I. INTRODUCTION

Solutions of the Schrödinger equation for $1/r^n$-type long-range potentials play a key role in quantum physics especially in the understanding of states, both bound and continuum, that are close to a threshold [1–4], and in the understanding of small-angle forward scattering which is dominated by contributions from large impact parameters. In the context of atomic collisions, it can be stated that cold atom collisions and highly excited molecular vibration spectra can be described by the solution of the Schrödinger equation for the proper long-range potential plus a few parameters that characterize the interactions of a shorter range [5–8].

For a potential that is asymptotically a repulsive $1/r^n$, the importance of the pure long-range solution becomes even more profound. The repulsive nature of the potential keeps the particles away from each other so that unless the energy is sufficiently large, the particles do not ''see'' the interactions at the short range and scattering is described by the *pure* $1/r^n$ solution over a wide range of energies.

The $1/r^3$ interaction, of which the repulsive case is studied in detail here, represents the radial dependence of resonant electric dipole-dipole, magnetic dipole-dipole, and quadrupole-monopole interactions. It plays an important role in many physical processes including collisions of similar atoms in a radiation field [9–12], molecular spectra converging to thresholds where two fragments can interact via resonant dipole-dipole interactions [13–23], and atom-surface interactions [24,25]. It is also important in the understanding of atom-electron and atom-ion interactions when the atom involved is in a state that possesses a permanent quadrupole moment.

Despite its significance, the $1/r^3$ interaction is one of the most poorly understood in the sense that it is the only long-range potential of the form of $1/r^n$ (n being a positive integer) for which even the threshold behavior has not been rigorously derived [26–28]. Mathematically, this difficulty originates from the fact that the radial Schrödinger equation for a potential of the form of $1/r^n$ with $n>2$ has two irregular singularities, one at $r=0$ and the other at $r=\infty$. A second-order differential equation of this type cannot be solved by a straightforward application of the power-series expansion that gave the Coulomb and harmonic-oscillator solutions.

Using methods that have been developed through the solutions of $1/r^4$ [29] and $1/r^6$ potentials [5], analytic solutions for both the attractive [8] and repulsive $1/r^3$ interactions have been obtained. The repulsive solutions presented here give an in-depth understanding of the scattering by a pure repulsive $1/r^3$ interaction in terms of a set of universal functions that are independent of both the reduced mass and the C_3 coefficient. The summary of the solution is presented in Sec. II with derivation given in Appendix A. Application to the pure repulsive $1/r^3$ scattering is discussed in Sec. III. Scattering by a potential which is only asymptotically a $+1/r^3$ is discussed in Sec. IV. Discussions of the threshold behavior and other issues are presented in Secs. V, and conclusions are given in Sec. VI.

II. THE REPULSIVE $1/r^3$ SOLUTIONS

Consider the radial Schrödinger equation for a $\mp C_3/r^n$ potential

$$\left[\frac{d^2}{dr^2}-\frac{l(l+1)}{r^2}\pm\frac{\beta_3}{r^3}+\bar{\epsilon}\right]u_l(r)=0, \tag{1}$$

where $\bar{\epsilon}\equiv 2\mu\epsilon/\hbar^2$, β_3 is a length scale defined by

$$\beta_3\equiv 2\mu C_3/\hbar^2, \tag{2}$$

and the plus and minus signs correspond to the attractive and the repulsive interactions, respectively.

Using a similar method that led to the $1/r^6$ solutions [29,5] (see Appendix A), we have found for a repulsive $1/r^3$ potential that a pair of linearly independent solutions with energy-independent behavior near the origin ($r\ll\beta_3$) can be written as

$$f^0_{\epsilon l}(r)=\frac{1}{\sin(2\pi\nu)}\{[F_{\epsilon l}(-\nu)]^{-1}\xi_{\epsilon l}-[F_{\epsilon l}(\nu)]^{-1}\eta_{\epsilon l}\}, \tag{3}$$

$$g^0_{\epsilon l}(r)=-\{[F_{\epsilon l}(-\nu)]^{-1}\xi_{\epsilon l}+[F_{\epsilon l}(\nu)]^{-1}\eta_{\epsilon l}\}, \tag{4}$$

where ξ and η are another pair of linearly independent solutions given by

$$\xi_{\epsilon l}(r)=\sum_{m=-\infty}^{\infty} b_m r^{1/2}J_{\nu+m}(\bar{\epsilon}^{1/2}r), \tag{5}$$

$$\eta_{\epsilon l}(r)=\sum_{m=-\infty}^{\infty}(-1)^m b_m r^{1/2} J_{-\nu-m}(\overline{\epsilon}^{1/2}r), \tag{6}$$

$$b_j=\Delta^j\frac{\Gamma(\nu)\Gamma(\nu-\nu_0+1)\Gamma(\nu+\nu_0+1)}{\Gamma(\nu+j)\Gamma(\nu-\nu_0+j+1)\Gamma(\nu+\nu_0+j+1)}c_j(\nu), \tag{7}$$

$$b_{-j}=\Delta^j\frac{\Gamma(\nu-j+1)\Gamma(\nu-\nu_0-j)\Gamma(\nu+\nu_0-j)}{\Gamma(\nu+1)\Gamma(\nu-\nu_0)\Gamma(\nu+\nu_0)}c_j(-\nu). \tag{8}$$

In Eqs. (7) and (8), j is a positive integer, and

$$\Delta=(\overline{\epsilon})^{1/2}\beta_3/2, \tag{9}$$

$$\nu_0=l+1/2, \tag{10}$$

$$c_j(\nu)=b_0Q(\nu)Q(\nu+1)\cdots Q(\nu+j-1). \tag{11}$$

The coefficient b_0 is a normalization constant which can be set to 1, and $Q(\nu)$ is given by a continued fraction

$$Q(\nu)=\cfrac{1}{1-\epsilon_s\cfrac{1}{(\nu+1)[(\nu+1)^2-\nu_0^2](\nu+2)[(\nu+2)^2-\nu_0^2]}Q(\nu+1)}, \tag{12}$$

where ϵ_s is a scaled energy defined by

$$\epsilon_s=\Delta^2=\frac{1}{4}\frac{\epsilon}{(\hbar^2/2\mu)(1/\beta_3)^2}. \tag{13}$$

The $F_{\epsilon l}(\nu)$ in Eqs. (3) and (4) is defined by

$$F_{\epsilon l}(\nu)=\Delta^{-\nu}\frac{\Gamma(1+\nu_0+\nu)\Gamma(1-\nu_0+\nu)}{\Gamma(1-\nu)}C(\nu), \tag{14}$$

where $C(\nu)=\lim_{j\to\infty}c_j(\nu)$.

Finally, ν is a root, which can be complex, of a characteristic function

$$\Lambda_l(\nu;\epsilon_s)\equiv(\nu^2-\nu_0^2)-(\epsilon_s/\nu)[\overline{Q}(\nu)-\overline{Q}(-\nu)]. \tag{15}$$

Here $\overline{Q}$ is defined by

$$\overline{Q}(\nu)\equiv\{(\nu+1)[(\nu+1)^2-\nu_0^2]\}^{-1}Q(\nu), \tag{16}$$

and can be conveniently evaluated [30] as a continued fraction

$$\overline{Q}(\nu)=\cfrac{1}{(\nu+1)[(\nu+1)^2-\nu_0^2]-\epsilon_s\overline{Q}(\nu+1)}. \tag{17}$$

The pair of solutions f^0 and g^0 has been defined in such a way that they have energy-independent behavior near the origin $(r/\beta_3\ll 1)$ characterized by

$$f^0_{\epsilon l}(r)\overset{r\to 0}{\to}\pi^{-1/2}r^{1/2}(r/\beta_3)^{1/4}\exp(-2(r/\beta_3)^{-1/2}), \tag{18}$$

$$g^0_{\epsilon l}(r)\overset{r\to 0}{\to}-\pi^{-1/2}r^{1/2}(r/\beta_3)^{1/4}\exp(2(r/\beta_3)^{-1/2}), \tag{19}$$

for both positive and negative energies. The solution f^0, which goes to zero in the limit of $r\to 0$, is thus the regular solution that satisfies the boundary condition at the origin.

The asymptotic behaviors of f^0 and g^0 at large r are given for $\epsilon>0$ by

$$f^0_{\epsilon l}(r)\overset{r\to\infty}{\to}\left(\frac{2}{\pi k}\right)^{1/2}\left[Z_{ff}\sin\left(kr-\frac{l\pi}{2}\right)-Z_{fg}\cos\left(kr-\frac{l\pi}{2}\right)\right], \tag{20}$$

$$g^0_{\epsilon l}(r)\overset{r\to\infty}{\to}\left(\frac{2}{\pi k}\right)^{1/2}\left[Z_{gf}\sin\left(kr-\frac{l\pi}{2}\right)-Z_{gg}\cos\left(kr-\frac{l\pi}{2}\right)\right], \tag{21}$$

where $k=(2\mu\epsilon/\hbar^2)^{1/2}$, and

$$Z_{ff}(\epsilon_s)=-\frac{\cos(\pi(\nu-\nu_0)/2)}{G_{\epsilon l}(-\nu)\sin 2\pi(\nu-\nu_0)}\times\left\{\left[1+(-1)^l M_{\epsilon l}\tan\frac{1}{2}\pi(\nu-\nu_0)\right]X_{\epsilon l}-\left[\tan\frac{1}{2}\pi(\nu-\nu_0)+(-1)^l M_{\epsilon l}\right]Y_{\epsilon l}\right\}, \tag{22}$$

$$Z_{fg}(\epsilon_s)=-\frac{\cos(\pi(\nu-\nu_0)/2)}{G_{\epsilon l}(-\nu)\sin 2\pi(\nu-\nu_0)}\times\left\{\left[\tan\frac{1}{2}\pi(\nu-\nu_0)+(-1)^l M_{\epsilon l}\right]X_{\epsilon l}+\left[1+(-1)^l M_{\epsilon l}\tan\frac{1}{2}\pi(\nu-\nu_0)\right]Y_{\epsilon l}\right\}, \tag{23}$$

$$Z_{gf}(\epsilon_s)=-\frac{\cos(\pi(\nu-\nu_0)/2)}{G_{\epsilon l}(-\nu)}\left\{\left[1-(-1)^l M_{\epsilon l}\times\tan\frac{1}{2}\pi(\nu-\nu_0)\right]X_{\epsilon l}-\left[\tan\frac{1}{2}\pi(\nu-\nu_0)-(-1)^l M_{\epsilon l}\right]Y_{\epsilon l}\right\}, \tag{24}$$

$$Z_{gg}(\epsilon_s)=-\frac{\cos(\pi(\nu-\nu_0)/2)}{G_{\epsilon l}(-\nu)}\left\{\left[\tan\frac{1}{2}\pi(\nu-\nu_0)-(-1)^l M_{\epsilon l}\right]X_{\epsilon l}+\left[1-(-1)^l M_{\epsilon l}\times\tan\frac{1}{2}\pi(\nu-\nu_0)\right]Y_{\epsilon l}\right\}, \tag{25}$$

where

$$G_{\epsilon l}(\nu)=|\Delta|^{-\nu}\frac{\Gamma(1+\nu_0+\nu)\Gamma(1-\nu_0+\nu)}{\Gamma(1-\nu)}C(\nu), \tag{26}$$

$$M_{\epsilon l}=G_{\epsilon l}(-\nu)/G_{\epsilon l}(\nu), \tag{27}$$

$$X_{\epsilon l}=\sum_{m=-\infty}^{\infty}(-1)^m b_{2m}, \tag{28}$$

$$Y_{\epsilon l}=\sum_{m=-\infty}^{\infty}(-1)^m b_{2m+1}. \tag{29}$$

For $\epsilon<0$, f^0 and g^0 have asymptotic behaviors at large r given by

$$f^0_{\epsilon l}(r)\overset{r\to\infty}{\to}(2\pi\kappa)^{-1/2}[W_{f-}e^{\kappa r}-W_{f+}(2e^{-\kappa r})], \tag{30}$$

$$g^0_{\epsilon l}(r)\overset{r\to\infty}{\to}(2\pi\kappa)^{-1/2}[W_{g-}e^{\kappa r}-W_{g+}(2e^{-\kappa r})], \tag{31}$$

where $\kappa=(2\mu|\epsilon|/\hbar^2)^{1/2}$,

$$W_{f-}(\epsilon_s)=-[G_{\epsilon l}(-\nu)\sin 2\pi(\nu-\nu_0)]^{-1}(1-M_{\epsilon l})D_{\epsilon l}, \tag{32}$$

$$W_{f+}(\epsilon_s)=-(-1)^l[2G_{\epsilon l}(-\nu)\sin 2\pi(\nu-\nu_0)]^{-1}\times\cos\pi(\nu-\nu_0)(1+M_{\epsilon l})E_{\epsilon l}, \tag{33}$$

$$W_{g-}(\epsilon_s)=-[G_{\epsilon l}(-\nu)]^{-1}(1+M_{\epsilon l})D_{\epsilon l}, \tag{34}$$

$$W_{g+}(\epsilon_s)=-(-1)^l[2G_{\epsilon l}(-\nu)]^{-1}\cos\pi(\nu-\nu_0)\times(1-M_{\epsilon l})E_{\epsilon l}, \tag{35}$$

$$D_{\epsilon l}=\sum_{m=-\infty}^{\infty}d_m, \tag{36}$$

$$E_{\epsilon l}=\sum_{m=-\infty}^{\infty}(-1)^m d_m, \tag{37}$$

and

$$d_j=(-|\Delta|)^j\times\frac{\Gamma(\nu)\Gamma(\nu-\nu_0+1)\Gamma(\nu+\nu_0+1)}{\Gamma(\nu+j)\Gamma(\nu-\nu_0+j+1)\Gamma(\nu+\nu_0+j+1)}c_j(\nu), \tag{38}$$

$$d_{-j}=|\Delta|^j\frac{\Gamma(\nu-j+1)\Gamma(\nu-\nu_0-j)\Gamma(\nu+\nu_0-j)}{\Gamma(\nu+1)\Gamma(\nu-\nu_0)\Gamma(\nu+\nu_0)}c_j(-\nu). \tag{39}$$

The χ function [5,6], which will be useful in a multichannel formulation [8], is defined by

$$\chi_l(\epsilon_s)\equiv W_{f-}/W_{g-}=[\sin 2\pi(\nu-\nu_0)]^{-1}\frac{1-M_{\epsilon l}}{1+M_{\epsilon l}}, \tag{40}$$

and the factor of 2 in front of $e^{-\kappa r}$ in Eqs. (30) and (31) has been introduced to normalize the determinant of the W matrix to 1.

The Z and the W matrices, as well as the χ function for a specific l, are all universal functions of ϵ_s which are independent of either the reduced mass or the C_3 coefficient. Different values of C_3 and μ only rescale the energy according to Eqs. (13) and (2).

From Eqs. (18) and (19), it is easy to show that the f^0 and g^0 pair has a Wronskian given by

$$W(f^0,g^0)=2/\pi. \tag{41}$$

Since the Wronskian is a constant that is independent of r, the asymptotic forms of f^0 and g^0 at large r should give the same result, which requires

$$\det(Z)=Z_{ff}Z_{gg}-Z_{gf}Z_{fg}=1, \tag{42}$$

$$\det(W)=W_{f-}W_{g+}-W_{g-}W_{f+}=1. \tag{43}$$

These relationships have been verified in our calculations.

III. SCATTERING BY A PURE REPULSIVE $1/r^3$ POTENTIAL

For a pure repulsive $1/r^3$ potential, the solution which satisfies the boundary condition at $r=0$ is the regular solution f^0. For $\epsilon>0$, its asymptotic behavior at infinity, Eq. (20), gives the K matrix

$$K_l\equiv\tan\delta_l^{(3+)}=-Z_{fg}/Z_{ff}=-\left\{\left[\tan\frac{1}{2}\pi(\nu-\nu_0)+(-1)^l M_{\epsilon l}\right]X_{\epsilon l}+\left[1+(-1)^l M_{\epsilon l}\tan\frac{1}{2}\pi(\nu-\nu_0)\right]Y_{\epsilon l}\right\}\times\left\{\left[1+(-1)^l M_{\epsilon l}\tan\frac{1}{2}\pi(\nu-\nu_0)\right]X_{\epsilon l}-\left[\tan\frac{1}{2}\pi(\nu-\nu_0)+(-1)^l M_{\epsilon l}\right]Y_{\epsilon l}\right\}^{-1}, \tag{44}$$

from which all scattering properties can be derived. For example, the partial cross section for angular momentum l is given by

$$\sigma_l/(\pi\beta_3^2)=(2l+1)\left[\frac{1}{\epsilon_s}\frac{K_l^2}{1+K_l^2}\right]. \tag{45}$$

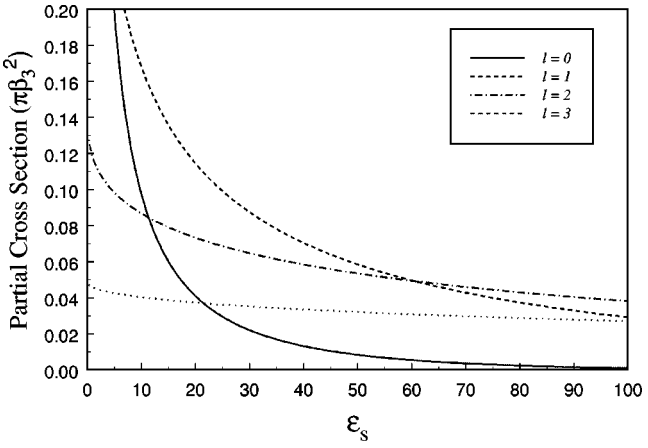

FIG. 1. Partial cross section vs scaled energy for $l=0,1,2,3$.

Figure 1 shows the energy dependencies of the partial cross sections for $l=0,1,2,3$. Figure 2 shows the energy dependencies of the partial cross sections for $l=4,5,6,7$. Figure 3 shows the energy dependencies of the total scattering cross sections summed over all l (the summation of cross sections from a large l to $l=\infty$ is discussed in Sec. V).

Note that with proper scaling of energy, the cross sections scaled by $\pi\beta_3^2$ are independent of either the C_3 coefficient or the reduced mass just like the Z matrix given by Eqs. (22)–(25). In other words, they are universal properties applicable to all pure repulsive $1/r^3$ interactions.

With the definitions

$$\tan\phi_l^{(1)} = -Y_{\epsilon l}/X_{\epsilon l}, \tag{46}$$

$$\tan\phi_l^{(2)} = -\frac{\tan(\pi(\nu-\nu_0)/2)+(-1)^l M_{\epsilon l}}{1+(-1)^l M_{\epsilon l}\tan(\pi(\nu-\nu_0)/2)}, \tag{47}$$

the scattering phase shift for a pure repulsive $1/r^3$ interaction can also be understood as the sum of $\phi_l^{(1)}$ and $\phi_l^{(2)}$,

$$\delta_l^{(3+)} = \phi_l^{(1)} + \phi_l^{(2)}. \tag{48}$$

Figure 4 shows the energy dependence of the s-wave phase shift along with respective contributions from $\phi_l^{(1)}$ and $\phi_l^{(2)}$.

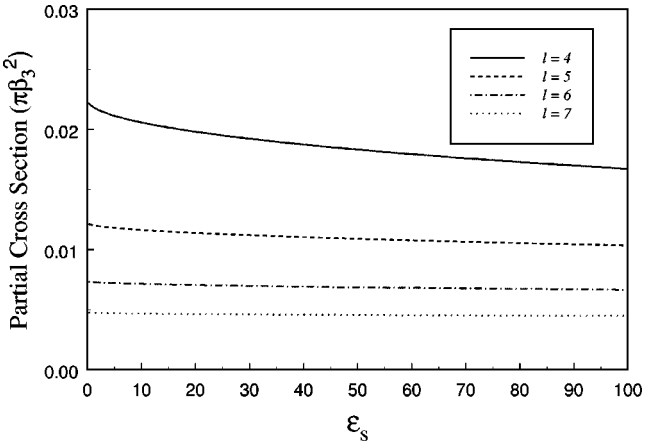

FIG. 2. Partial cross section vs scaled energy for $l=4,5,6,7$.

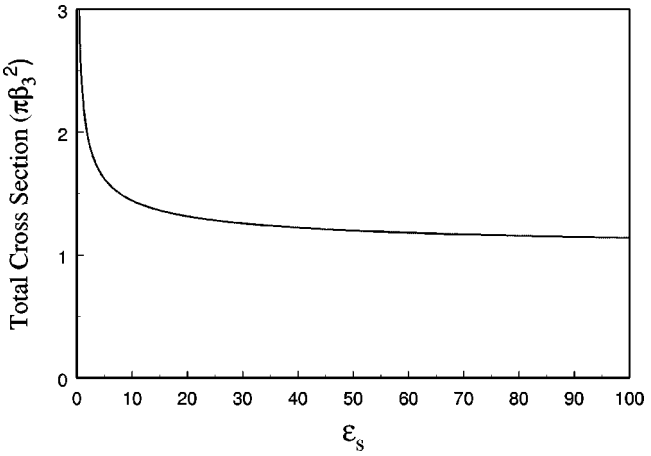

FIG. 3. Total scattering cross section vs scaled energy for a repulsive $1/r^3$ interaction.

IV. SCATTERING BY A POTENTIAL WHICH IS ASYMPTOTICALLY A REPULSIVE $1/r^3$

If the potential is repulsive and varies as $1/r^3$ only beyond a certain range r_0, the wave function which satisfies the boundary condition at the origin is no longer f^0. In particular, its behavior in the region of $r \geqslant r_0$ is now characterized by a linear superposition with both an f^0 and g^0 component,

$$u_{\epsilon l}(r) = A_{\epsilon l}[f_{\epsilon l}^0(r) - K_l^0 g_{\epsilon l}^0(r)]. \tag{49}$$

Here $A_{\epsilon l}$ is a normalization constant and K_l^0 is a short-range K matrix which depends only on the interactions of a shorter range. It is obtained by matching to the inner solution and is related to the logarithmic derivative of the wave function by

$$K_l^0 = \left(\frac{f_{\epsilon l}^0}{g_{\epsilon l}^0}\right)\frac{(f_{\epsilon l}^{0\prime}/f_{\epsilon l}^0)-(u_{\epsilon l}'/u_{\epsilon l})}{(g_{\epsilon l}^{0\prime}/g_{\epsilon l}^0)-(u_{\epsilon l}'/u_{\epsilon l})}. \tag{50}$$

The short-range K matrix K_l^0 is generally r-dependent. It converges to a constant when the potential becomes well represented by a pure $+1/r^3$. This radius of convergence is the more rigorous definition of r_0, applicable even when there are other $1/r^n$-type corrections to $+1/r^3$.

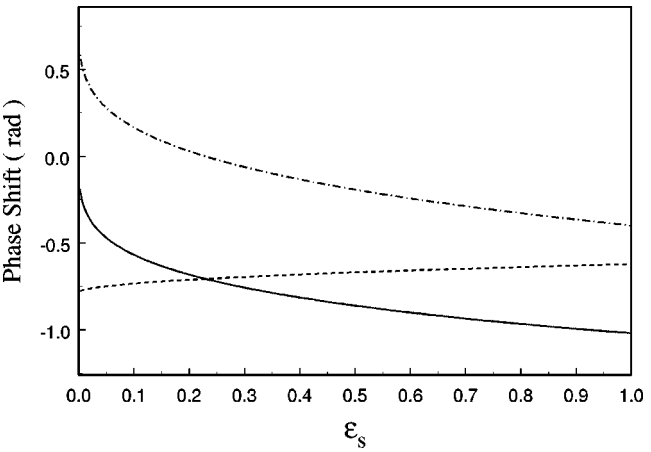

FIG. 4. s wave phase shift vs scaled energy for a pure repulsive $1/r^3$ interaction. Solid line: s wave phase shift. Dashed line: contribution from $\phi_l^{(1)}$. Dash-dotted line: contribution from $\phi_l^{(2)}$.

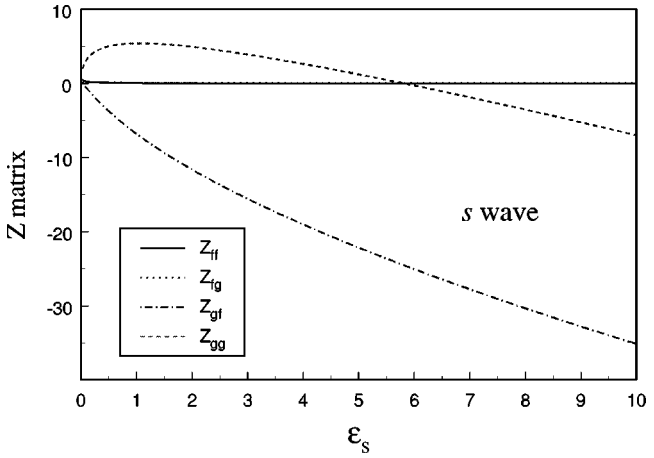

FIG. 5. The elements of the Z matrix for the s wave.

From the asymptotic behaviors of f^0 and g^0 as given in Eqs. (20) and (21), it is straightforward to extract from the asymptotic behavior of $u_{\epsilon l}$ that

$$K_l \equiv \tan\delta_l = (K_l^0 Z_{gg} - Z_{fg})(Z_{ff} - K_l^0 Z_{gf})^{-1}. \qquad (51)$$

This is the same quantum defect formulation for the scattering phase shift as previously presented for the $1/r^6$ interaction [5,6]. It serves the purpose of separating the effects of the long-range interaction from the interactions of a shorter range and separating common properties shared by large classes of systems (all systems with $+1/r^3$ asymptotic behavior have the same Z functions with only the energy scaling being different) from system-specific properties (different systems have different K_l^0). This separation is especially useful when the long-range interaction is strong as measured by $\beta_n \gg r_0$, in which case K_l^0 varies with energy much more slowly compared to the energy variations of Z [6]. Figures 5 and 6 are plots of the elements of the Z matrices for s and p waves, respectively.

What makes the repulsive $1/r^3$ interaction interesting and easier to deal with is that K^0 is well approximated by zero over a range of energies around the threshold. More precisely, if the long-range repulsion is sufficiently strong and the energy is sufficiently small so that the potential deviates from the pure $1/r^3$ form only in the classically forbidden region, it easy to show from Eqs. (18), (19), and (50) that K^0 is exponentially small. In other words, the scattering in this case is well approximated by a *pure* $+1/r^3$ interaction. This is the mathematical correspondence of the physical expectation that the repulsive potential keeps the colliding fragments apart so that they can hardly ''see'' the interactions at the short range except for large energies.

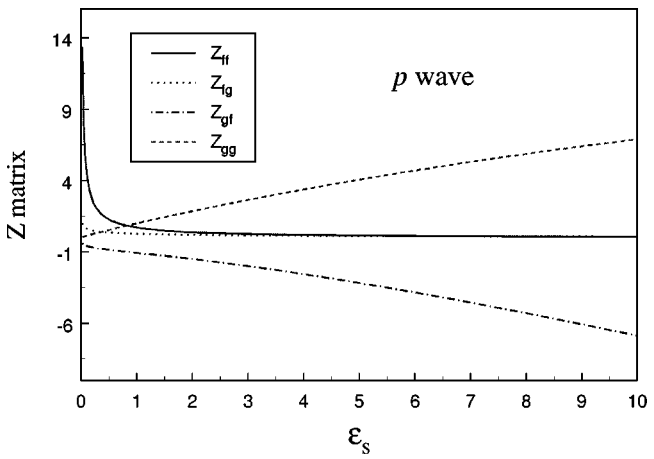

FIG. 6. The elements of the Z matrix for the p wave.

TABLE I. Critical scaled energies for $\epsilon > 0$ and different angular momentum l. ν becomes complex for $\epsilon > \epsilon_{sc}^{(+)}$.

l	$\epsilon_{sc}^{(+)}(l)$	$(\epsilon_{sc}^{(+)})^{1/6}$
0	2.529016×10^{-2}	0.5417829
1	1.585220×10^{0}	1.079812
2	1.736149×10^{1}	1.609155
3	9.700576×10^{1}	2.143547
4	3.725395×10^{2}	2.682432
5	1.123821×10^{3}	3.224404
6	2.863254×10^{3}	3.768281
7	6.437897×10^{3}	4.313111
8	1.314596×10^{4}	4.858088
9	2.486313×10^{4}	5.402474
10	4.417229×10^{4}	5.945545

V. DISCUSSIONS

A. Computation

In computing the scattering properties and in a more general quantum defect formulation [1,2,6,8], the key quantities to calculate are the Z matrix and the χ function. The computation is for the most part straightforward except one needs to keep in mind that the roots of the characteristic function, i.e., the proper ν to be used, can move into the complex plane.

The characteristic function $\Lambda_l(\nu;\epsilon_s)$ defined by Eq. (15) is a function of ν with ϵ_s as a parameter. It can be calculated to the desired precision by using the continued fraction expression for $\overline{Q}(\nu)$ as given by Eq. (17) and following the standard computational procedures [30]. The roots of Λ_l have the following properties for $\epsilon_s \neq 0$: (i) if ν is a solution, then $-\nu$ is also a solution; (ii) if ν is a solution, then ν^* is also a solution; and (iii) if ν is a noninteger solution, then $\pm\nu + n$ where n is an integer is also a solution. These properties are consistent with the Neumann expansion and are similar to the case of the $1/r^6$ potential [5]. For $\epsilon_s > 0$, it can be shown that the roots of Λ_l become complex beyond a critical scaled energy ϵ_{sc} determined by the solution of

$$\Lambda_l(\nu=0;\epsilon_s) = -\nu_0^2 - 2\epsilon_s \overline{Q}'(\nu=0) = 0. \qquad (52)$$

This critical scaled energy corresponds to the ϵ_s at which a pair of roots of Λ_l coalesces at an integer value and moves subsequently into the complex plane to become a pair which are complex conjugate of each other. Both ν and ν^* give the same physical results, and we will take the one with the positive imaginary part. Table I lists the critical scaled energies $\epsilon_{sc}^{(+)}$ for the first 11 partial waves.

With proper definitions of the Z and the W matrices, such as the way they are defined in Sec. II, all of their elements

remain real even when ν is in the complex plane. This is a key check on the validity and the accuracy of numerical calculations.

B. Energy-normalized solutions

For a pure repulsive $1/r^3$ potential, the energy-normalized regular solution is

$$u_{\epsilon l}(r)=\mathcal{N}_l(\epsilon_s)f^0_{\epsilon l}(r), \tag{53}$$

where

$$\mathcal{N}_l(\epsilon_s)=\cos\delta_l^{(3+)}(Z_{ff})^{-1}. \tag{54}$$

It satisfies the boundary condition at the origin and is energy-normalized with asymptotic behavior at large r given by

$$u_{\epsilon l}(r)\overset{r\to\infty}{\to}\left(\frac{2}{\pi k}\right)^{1/2}\sin\left(kr-\frac{l\pi}{2}+\delta_l^{(3+)}\right), \tag{55}$$

where $\tan\delta_l^{(3+)}$ is given by Eq. (44).

If the potential is $+1/r^3$ only beyond a radius r_0, the energy-normalized regular solution is given for $r\geqslant r_0$ by

$$u_{\epsilon l}(r)=\mathcal{N}_l(\epsilon_s)[f^0_{\epsilon l}(r)-K_l^0 g^0_{\epsilon l}(r)], \tag{56}$$

with

$$\mathcal{N}_l(\epsilon_s)=\cos\delta_l(Z_{ff}-K_l^0 Z_{gf})^{-1}. \tag{57}$$

It has an asymptotic behavior characterized by

$$u_{\epsilon l}(r)\overset{r\to\infty}{\to}\left(\frac{2}{\pi k}\right)^{1/2}\sin\left(kr-\frac{l\pi}{2}+\delta_l\right), \tag{58}$$

where $\tan\delta_l$ is given by Eq. (51).

The expression of energy normalized solutions in terms of f^0 and g^0 facilitates the understanding of energy dependencies of the matrix elements between different states [2]. For example, the normalization factor given by Eq. (54) would characterize the energy dependence of the Frank-Condon overlap between a pure repulsive $1/r^3$ continuum state and a state which is localized in the region of $r\ll\beta_3$ (since f^0 itself is independent of energy in this region). Figure 7 is a plot of $|\mathcal{N}_l(\epsilon_s)|$ versus the scaled energy for s, p, and d partial waves.

C. Threshold behavior

The threshold behavior for a repulsive $1/r^3$ interaction is given by the small ϵ_s expansion of Eq. (51). To the order of $(k\beta_3)$, we obtain

$$\tan\delta_{l=0}=\frac{(k\beta_3)\ln(k\beta_3)+[3\gamma+\ln 2-(3/2)](k\beta_3)}{1+(k\beta_3)\ln(k\beta_3)+[3\gamma+\ln 2-(13/6)-(\pi/2)](k\beta_3)}, \tag{59}$$

$$\tan\delta_{l\geqslant 1}=-\frac{1}{2l(l+1)}(k\beta_3), \tag{60}$$

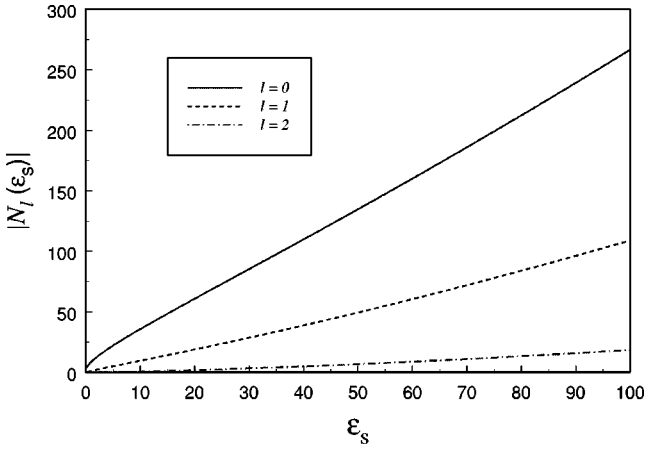

FIG. 7. $|\mathcal{N}_l(\epsilon_s)|$ for a pure repulsive $1/r^3$ potential. It represents, for example, the energy dependence of the Frank-Condon overlap between a pure repulsive $1/r^3$ continuum state and a state which is localized in the region of $r\ll\beta_3$.

where $\gamma=0.577\,215\,664\,9\ldots$ is Euler's constant [31]. In the limit of energy going to zero, the s-wave phase shift goes to zero but the partial cross section diverges logarithmically according to

$$\sigma_{l=0}/(\pi\beta_3^2)\overset{\epsilon_s\to 0}{\to}4[\ln(k\beta_3)]^2. \tag{61}$$

The cross sections for other partial waves go to a constant according to

$$\sigma_{l\geqslant 1}/(\pi\beta_3^2)\overset{\epsilon_s\to 0}{\to}1/l^2-1/(l+1)^2. \tag{62}$$

In comparison, the partial cross sections for a $1/r^2$ potential diverge according to $1/\epsilon$ for all l. For a $1/r^n$ potential with $n>3$, the s wave partial cross section goes to a constant and the cross sections for other partial waves go to zero in the limit of zero energy [26,27].

Even though Eqs. (59) and (60) represent the expansions to the same order of $(k\beta_3)$ for all l, their ranges of applicability are very different for different l. Figure 8 shows that

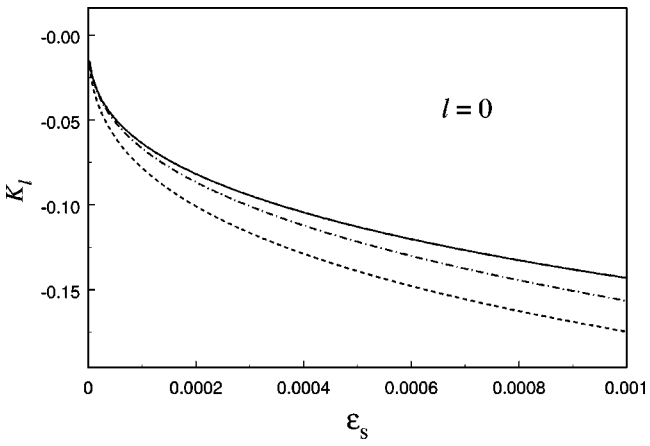

FIG. 8. Comparison of threshold expansions and the exact result of $\tan\delta_l$ for the s wave. Solid line: exact result. Dash-dotted line: approximation given by Eq. (59). Dashed line: the simple approximation $\tan\delta_l=(k\beta_3)\ln(k\beta_3)$.

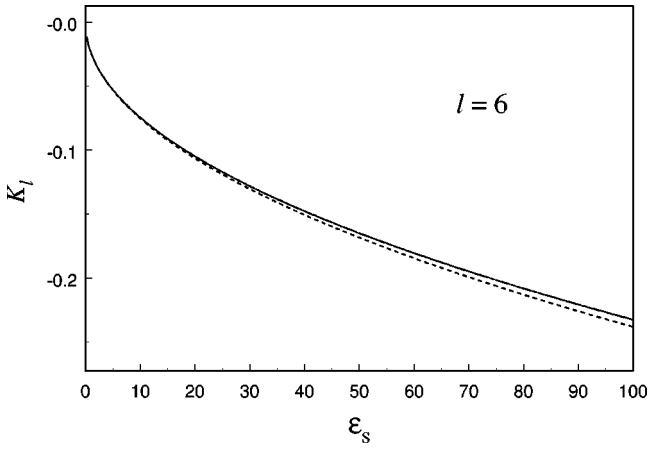

FIG. 9. Comparison of the threshold expansion and the exact result of $\tan\delta_l$ for $l=6$. Solid line: exact result. Dashed line: approximation given by Eq. (59).

the approximation given by Eq. (59) is applicable only for a very small range of energies around the threshold, especially if one keeps only the $(k\beta_3)\ln(k\beta_3)$ term. In contrast, Fig. 9 shows that Eq. (60), when used for a larger $l=6$, is accurate over a much greater range of energies. The reason for this vastly different range of applicability is that Eq. (60) is not only a small energy expansion, it is also a large l expansion. It is applicable regardless of energy for sufficiently large l. Thus the criterion for the validity of the threshold expansion is not $k\beta_3 \ll 1$. It is determined instead by

$$\epsilon_s \ll \epsilon_{sc}^{(+)}(l), \tag{63}$$

a condition under which ν has not moved far from ν_0. From the values of $\epsilon_{sc}^{(+)}$ given in Table I, one can see that the threshold expansion for large l works over a much greater energy range than the corresponding expansion for small l.

Since $\tan\delta_l$ can be calculated exactly, the threshold approximations given by Eqs. (59) and (60) are generally not recommended except for conceptual purposes. The exception is the use of Eq. (60) for sufficiently large l. In particular, it can be used to sum up the large l contributions at any energy. For example, letting l_m be the angular momentum beyond which the condition, Eq. (63), is well satisfied, Eq. (60) leads immediately to

$$\sum_{l=l_m}^{\infty} \sigma_l/(\pi\beta_3^2) = 1/l_m^2. \tag{64}$$

D. Comparison with the attractive $1/r^3$ potential

As one would expect, solutions for repulsive and attractive $1/r^3$ interactions are similar mathematically, as discussed in more detail in a separate paper on the attractive interaction [8] which will soon be submitted. The physical behavior described by the two types of interactions is, however, vastly different. In particular, we emphasize that a pure attractive $1/r^3$ potential does not constitute a meaningful quantum system by itself since the corresponding Schrödinger equation does not have a solution which can satisfy the boundary condition at $r=0$. This is true for any attractive potential of the type of $1/r^n$ with $n>2$ [5]. For these types of systems, the $-1/r^n$ solutions always have to be matched to a proper inner solution to yield a meaningful wave function. In other words, a short-range parameter K^0 is always part of the theory [6], and the definition of a pure long-range phase shift is not meaningful.

In contrast, a quantum system with a pure repulsive $1/r^n$ interaction is well defined. A solution that satisfies the boundary condition at $r=0$ does exist, and a pure long-range phase shift, such as $\delta_l^{(3+)}$, can be introduced. Furthermore, because the repulsive nature of the potential keeps the particles apart, a *pure* repulsive $1/r^n$ potential can be a good approximation even when the inner part of the real potential deviates from it.

VI. CONCLUSION

Analytic solutions of the Schrödinger equation for a repulsive $1/r^3$ potential have been presented which lead to an in-depth understanding of scattering by a potential which is asymptotically a repulsive $1/r^3$. They have applications in many quantum systems where the repulsive $1/r^3$ interaction can be due to resonant electric dipole-dipole, magnetic dipole-dipole, or quadrupole-monopole interactions. In particular, these solutions, together with the $1/r^6$ solutions [5] and the attractive $1/r^3$ solutions [8], provide the foundation for a multichannel quantum defect formulation of slow atomic collisions and highly excited molecular vibration spectra [32,6–8]. In this formulation, both the collisional and the spectroscopical properties that are common to a wide class of systems are factored out and described analytically, while system-specific properties are characterized by a few parameters that depend weakly on energy. And with solutions for both the ground and the excited asymptotic potentials, processes such as cold collisions of similar atoms in a laser field [9–12] and photoassociative spectroscopy of similar atoms [14–23] can also be understood in a more systematic manner.

ACKNOWLEDGMENTS

I would like to thank Tom Kvale for helpful discussions and for reading the manuscript.

APPENDIX A: DERIVATION OF THE SOLUTIONS

The key steps in arriving at these solutions are parallel to those in the $1/r^6$ solutions [5]. First, a solution is expressed as a generalized Neumann expansion with proper argument so that the coefficients satisfy a three-term recurrence relation. Second, the recurrence relations are solved using continued fractions. Third, the asymptotic behavior near the origin is obtained by examining a corresponding Laurent-type expansion.

1. Change of variable

Through a change of variable defined by

$$x=(r/L)^{\alpha}, \tag{A1}$$

$$u_l(r)=r^{1/2}f(x), \tag{A2}$$

with $\alpha=1$ and $L=(\bar{\epsilon})^{-1/2}$, Eq. (1) can be written as

$$\left[x^2\frac{d^2}{dx^2}+x\frac{d}{dx}+x^2-\nu_0^2\right]f(x)=2\Delta\frac{1}{x}f(x), \tag{A3}$$

in which $\Delta=(\bar{\epsilon})^{1/2}\beta_3/2$ and $\nu_0=l+1/2$. Except for the different definitions of x, Δ, and ν_0, and a different sign on the right-hand side, this equation is identical to Eq. (34) of [5], and is solved in the same fashion in terms of the Neumann expansion and continued fractions [29,5]. The result is the pair of solutions given by Eqs. (5) and (6).

2. Asymptotic behaviors

The asymptotic behaviors of solutions at large r are straightforward. From the asymptotic expansions of the Bessel functions for large arguments [31], we obtain for $\epsilon<0$ $(\Delta=i\kappa\beta_3/2)$

$$\Delta^{-\nu}\xi_{\epsilon l}\overset{r\to\infty}{\to}|\Delta|^{-\nu}(2\pi\kappa)^{-1/2}(D_{\epsilon l}e^{\kappa r}-E_{\epsilon l}\sin\pi\nu e^{-\kappa r}), \tag{A4}$$

$$\Delta^{\nu}\eta_{\epsilon l}\overset{r\to\infty}{\to}|\Delta|^{\nu}(2\pi\kappa)^{-1/2}(D_{\epsilon l}e^{\kappa r}+E_{\epsilon l}\sin\pi\nu e^{-\kappa r}), \tag{A5}$$

where $D_{\epsilon l}$ and $E_{\epsilon l}$ are defined in Eqs. (36) and (37). For $\epsilon>0$, the asymptotic behaviors at large r have the most symmetric form for the pair of functions

$$\bar{f}_{\epsilon l}(r)=\sum_{m=-\infty}^{\infty}b_m r^{1/2}J_{\nu+m}(\bar{\epsilon}^{1/2}r), \tag{A6}$$

$$\bar{g}_{\epsilon l}(r)=\sum_{m=-\infty}^{\infty}b_m r^{1/2}Y_{\nu+m}(\bar{\epsilon}^{1/2}r), \tag{A7}$$

which are related to ξ and η by

$$\bar{f}_{\epsilon l}(r)=\xi_{\epsilon l}(r), \tag{A8}$$

$$\bar{g}_{\epsilon l}(r)=\frac{1}{\sin(\pi\nu)}[\xi_{\epsilon l}\cos(\pi\nu)-\eta_{\epsilon l}]. \tag{A9}$$

The large r behavior of $\bar{f}$ and $\bar{g}$ is easily shown to be

$$\bar{f}_{\epsilon l}\overset{r\to\infty}{\to}(2/\pi k)^{1/2}[\alpha_{\epsilon l}\sin(kr-l\pi/2)-\beta_{\epsilon l}\cos(kr-l\pi/2)], \tag{A10}$$

$$\bar{g}_{\epsilon l}\overset{r\to\infty}{\to}(2/\pi k)^{1/2}[-\beta_{\epsilon l}\sin(kr-l\pi/2)-\alpha_{\epsilon l}\cos(kr-l\pi/2)], \tag{A11}$$

where

$$\alpha_{\epsilon l}=\cos(\pi(\nu-\nu_0)/2)X_{\epsilon l}-\sin(\pi(\nu-\nu_0)/2)Y_{\epsilon l}, \tag{A12}$$

$$\beta_{\epsilon l}=\sin(\pi(\nu-\nu_0)/2)X_{\epsilon l}+\cos(\pi(\nu-\nu_0)/2)Y_{\epsilon l}, \tag{A13}$$

with $X_{\epsilon l}$ and $Y_{\epsilon l}$ defined in Eqs. (28) and (29).

To derive the asymptotic behaviors at small r, we rewrite the ξ function as a Laurent-type expansion

$$\xi_{\epsilon l}(r)=r^{1/2}(z/2)^{-2\nu}\sum_{m=-\infty}^{\infty}p_m(z/2)^{2m}, \tag{A14}$$

where $z=2(r/\beta_3)^{-1/2}$ and

$$p_m=\Delta^{\nu}\sum_{s=0}^{\infty}\frac{(-1)^s}{s!\Gamma(\nu-m-s+1)}\Delta^{2s}[\Delta^{-(m+2s)}b_{-(m+2s)}]. \tag{A15}$$

The asymptotic behavior of ξ at large z (small r) depends only on the m dependence of p_m for large m [33]. Making use of the properties of the gamma function for large arguments [31] and the properties of b_{-j} for large j, one can show that

$$p_m\overset{m\to\infty}{\to}F_{\epsilon l}(-\nu)\frac{1}{m!\Gamma(-2\nu+m+1)}, \tag{A16}$$

where $F_{\epsilon l}(\nu)$ is defined by Eq. (14). Comparing the m dependence of p_m with the coefficients of the modified Bessel function [31], we have

$$\xi_{\epsilon l}\overset{r\to 0}{\to}F_{\epsilon l}(-\nu)r^{1/2}\lim_{r\to 0}I_{-2\nu}(2(r/\beta_3)^{-1/2}). \tag{A17}$$

Similarly for the η function we have

$$\eta_{\epsilon l}\overset{r\to 0}{\to}F_{\epsilon l}(\nu)r^{1/2}\lim_{r\to 0}I_{2\nu}(2(r/\beta_3)^{-1/2}). \tag{A18}$$

The asymptotic behaviors of f^0 and g^0 are easily derived from those presented in this section.

[1] M. J. Seaton, Rep. Prog. Phys. **46**, 167 (1983).
[2] U. Fano and A. R. P. Rau, *Atomic Collisions and Spectra* (Academic Press, Orlando, 1986), and references therein.
[3] C. H. Greene, A. R. P. Rau, and U. Fano, Phys. Rev. A **26**, 2441 (1982).
[4] C. H. Greene and L. Kim, Phys. Rev. A **38**, 5953 (1988), and references therein.
[5] B. Gao, Phys. Rev. A **58**, 1728 (1998).
[6] B. Gao, Phys. Rev. A **58**, 4222 (1998).
[7] J. P. Burke, Jr., C. H. Greene, and J. L. Bohn, Phys. Rev. Lett. **81**, 3355 (1998).
[8] B. Gao (unpublished).
[9] A. Gallagher and D. E. Pritchard, Phys. Rev. Lett. **63**, 957 (1989).
[10] P. S. Julienne, A. M. Smith, and K. Burnett, Adv. At., Mol., Opt. Phys. **30**, 141 (1992).

[11] K. Suominen, J. Phys. B **29**, 5981 (1996).
[12] C. Orzel, S. D. Bergeson, S. Kulin, and S. L. Rolston, Phys. Rev. Lett. **80**, 5093 (1998).
[13] W. C. Stwalley, Y. Uang, and G. Pichler, Phys. Rev. Lett. **41**, 1164 (1978).
[14] H. R. Thorsheim, J. Weiner, and P. S. Julienne, Phys. Rev. Lett. **58**, 2420 (1987).
[15] P. D. Lett *et al.*, Phys. Rev. Lett. **71**, 2200 (1993).
[16] J. D. Miller, R. A. Cline, and D. J. Heinzen, Phys. Rev. Lett. **71**, 2204 (1993).
[17] R. A. Cline, J. D. Miller, and D. J. Heinzen, Phys. Rev. Lett. **73**, 632 (1994).
[18] C. J. Williams and P. S. Julienne, J. Chem. Phys. **101**, 2634 (1994).
[19] L. P. Ratliff *et al.*, J. Chem. Phys. **101**, 2638 (1994).
[20] W. I. McAlexander *et al.*, Phys. Rev. A **51**, R871 (1995).
[21] E. R. I. Abraham *et al.*, J. Chem. Phys. **103**, 7773 (1995).
[22] K. M. Jones *et al.*, Europhys. Lett. **35**, 85 (1996).
[23] H. Wang, P. L. Gould, and W. C. Stwalley, Phys. Rev. A **53**, R1216 (1996).
[24] W. C. Stwalley, Chem. Phys. Lett. **88**, 404 (1982).
[25] A. Zangwill, *Physics at Surfaces* (Cambridge University Press, Cambridge, 1988), and references therein.
[26] B. R. Levy and J. B. Keller, J. Math. Phys. **4**, 54 (1963). A concise summary of their results can also be found in [27].
[27] P. G. Burke, *Potential Scattering in Atomic Physics* (Plenum Press, New York, 1977).
[28] For a $1/r^3$ potential, the effective-range expansion does not apply even for the *s* wave [26,27]. Levy and Keller did correctly *speculate* that the *s*-wave phase shift may have a leading behavior of $-k \ln k$ [26,27].
[29] M. J. Cavagnero, Phys. Rev. A **50**, 2841 (1994).
[30] W. H. Press *et al.*, *Numerical Recipes in C* (Cambridge University Press, Cambridge, 1992), and references therein.
[31] *Handbook of Mathematical Functions*, edited by M. Abramowitz and I. A. Stegun (National Bureau of Standards, Washington, D.C., 1964).
[32] B. Gao, Phys. Rev. A **54**, 2022 (1996).
[33] C. M. Bender and S. A. Orszag, *Advanced Mathematical Methods for Scientists and Engineers* (McGraw-Hill, New York, 1978).